Final Report

In this final report I summarize the main achievements/results of our activity in the frame of the OTKA 113222 project. In agreement with our commitments of the research plan our activity was concentrated on the research of the amplification properties of KrF excimer medium and of the corresponding amplification schemes in order to improve/raise the output parameters of our high-brightness UV system, with special emphasis on the maximum intensity (brightness) and intensity contrast.

Parallel with this activity, we also used this unique laser system of improving parameters for studying special laser-matter interactions and for pumping secondary light sources.

In the selection of these applications we preferred those; where the unique parameters of our light source play important role and/or the associated research field is in (or moved to) the centre of the interest of the research community.

Energy issues; amplifier research and development

The small saturation energy density of excimers (~ 2 mJ/cm^2) requires large amplifier geometries [1], which – in the conventional designs – are limited by the electrical requirements of discharge pumping [2,3]. This contradiction can only be relaxed/solved by the invention/use of novel concepts: by the so-called off-axis amplification scheme [4] and the back-to-back arrangement [5]. In these approaches the optically usable cross-section is increased by tilting the discharge with respect to the beam or matching two discharges.

Our amplifier development was concentrated on the research and development of gain modules whose optical and geometrical parameters are fitted to the requirements of these concepts.

1. In order to overcome the geometrical limitations on the optical cross-section (imposed by the limited discharge loop and by the short absorption length of UV preionization) a spark preionized, "orthogonal" multichannel gain module of 10x4.5 cm^2 effective cross-section was developed and realized. In this design several discharge-pumped "slabs" – oriented perpendicular to the beam – are used in sequence. In this way the beam "sees" the discharge from the side, thus eliminating the "conventional" limitations not only on the cross-section but also on the homogeneity. Our observations confirmed two drawbacks of this design:
   - the off-axis amplification cannot be used for the smaller dimension of the amplifier's aperture, because of the blocking effect of the electrodes,
   - along the optical axis of the beam there is a periodic spatial sequence of pumped and unpumped volumes, which decreases the effective gain coefficient.
2. Referring to the above listed drawbacks, a comparative study of two (an X-ray and UV preionized) large aperture KrF excimer amplifier designs were performed. For this reason a "quasi-conventional" X-ray preionized gain module of w/d ≈ 1 aspect-ratio (w is the width of the discharge, d is the electrode gap separation) and of large cross-section has been developed (accommodated to the special requirements of the off-axis amplification geometry and of the back-to-back design) [6].

This is based on the use of a 45 cm long flat and curved electrode pair of 4.5 cm gap separation, driven by a magnetic-switch-controlled charging circuit and preionized by a pencil-like, short-pulse X-ray tube.

As far as the requirements for the X-ray source are concerned; due to the very low absorption of X-ray in the gas mix, and the fast (several times 10 ns) relaxation of ions (by halogen attachment), effective ionization of the gas by a very short and very intense X-ray pulse is necessary [7]. For this reason we have developed

- a fast, HV power supply of 100 kV maximum voltage and ~20 ns risetime,
- an elongated, cold-cathode X-ray tube,
- an active synchronization unit, which actively controls the delay (with 5 ns accuracy) between preionization and the main discharge.

As a result, the discharge volume is illuminated by a well-synchronized X-ray pulse of ~16 ns duration. While the dose of the X-ray radiation (~100mR) is similar to that of former approaches – due to its short duration – it is ~10 times more intense, therefore to the same extent more effective, fulfilling the needs of sufficient preionization of the KrF mixture. The carbon-fiber based cathode allows very high (several 100 A/cm^2) peak current densities, and moderate tube cross-sections (~10cm^2). This X-ray gun design – due to its simplicity allows – to insert the preionization (actually two or even more X-ray guns) inside the discharge chamber. This is a very effective way of increasing the preionization rate at the position of the discharge (compared to the "external" X-ray preionization) by eliminating the absorption of X-rays occurring in the relatively thick discharge chamber, and reducing the spatial decrease of the X-ray intensity (scaling with 1/r for a cylindrical symmetry).

With regard to the symmetry of the discharge and to the requirements of the back-to-back design a double, line-emitting X-ray source is developed. In order to operate two synchronized X-ray guns, a special power supply has also been developed, which can drive two X-ray diodes simultaneously, while they do not interfere by electrical means.

We have realized a discharge unit, where the two elongated cylindrical X-ray guns are positioned inside the laser chamber, directly surrounding the main electrodes.

Beyond the significant increase of the X-ray intensity offered by this designs, there are two facts we found to be considered:

- Due to the comparable distance of the preionization source and the cross-sectional dimensions of the discharge, the spatial dependence of the X-ray intensity in the discharge volume becomes considerable. Its consequence is that not only the spatial distribution of the electric field, but also the spatial intensity of the X-ray radiation (together) determine the geometry of the discharge (including the optical cross-section of the amplifier).
- The cylindrical walls of the X-ray guns must fulfill even more requirements such as: excellent mechanical stability electric isolation, small X-ray absorption, resistivity against F2, ability to maintain clean surface.

For a relatively long time our activity was concentrated to find the optimum shape (and separation) of the main electrodes, which – together with the effect of the spatially dependent X-ray preionization – results in a homogeneous discharge of the necessary cross-section.

Parallel with these experiments several material/design was tested for the walls/tube of the X-ray gun, such as: glass, quartz, plexi glass, polyetilene, poly-vynil-difluoride, teflon and their combinations. Unfortunately none of them fulfilled all formerly listed requirements.

For these reasons we turned back to that approach, where the X-ray guns are placed outside the discharge chamber. In this design – in contrast to former approaches – two X-ray guns are positioned around the cathode electrode, and irradiation of the discharge volume is realized through the aluminium electrode. This approach has three advantages:

- the problems associated with the wall material of the X-ray guns are relaxed,
- the cathode section of the discharge volume is irradiated more efficiently (this region is the most sensitive for the level of preionization),
- change of the positions of the two X-ray guns can be used to "tune" the spatial distribution of the X-ray field in the discharge. Therefore the formerly used, more complicated tuning based on the change of the electrode separation can be avoided.

Former investigations showed that the spatial distribution of the discharge is the critical interplay of that of both the E-field and the preionization. For a given E-field distribution this makes, in principle possible to fine-tune the discharge geometry by proper control of the spatial characteristics of preionization.

This feature of X-ray preionization – based on two externally positioned X-ray guns – is proven both theoretically and experimentally. Fig. 1 shows the calculated spatial distribution of the X-ray radiation across the discharge area for three different positions of the X-ray sources; when preionization is done at the center (I), from two sides of the discharge (III) and from upper lying sources (from left and right hand). It is seen from the curves that the shape of the spatial distribution

of the strength of preionization can be tuned from convex to concave (through a flat distribution) by properly changing the positions of the line emitting preionizers. This, however, also "tunes" the discharge width (from 22 mm to 45 mm) giving a practical method to compensate for eventual inhomogeneities of the E-field of excitation and to tune the discharge to the desired geometry.

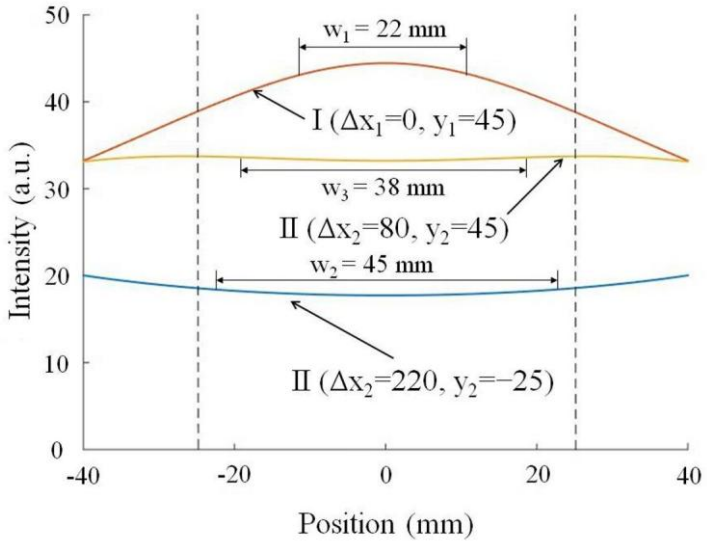

Figure 1 *Calculated distribution of the X-ray intensity, when preionization is done I) by one X-ray source from above (through the electrode), II) by two X-ray sources from two sides (through the walls) and III) by two X-ray sources, properly positioned above the cathode electrode. Along the curves the experimentally obtained discharge widths (w) are also indicated*

As a result of this fine tuning of preionization a short-pulse KrF excimer gain module of homogeneous ~ 20 cm^2 cross-section is developed offering ~ 200 mJ momentarily stored energy. This allows > 200 mJ short-pulse energy in a two beam interferometric multiplexing geometry (as used in our presently operational short-pulse laser system but for a ~ 8 cm^2 gain module, shown in Fig. 5 of this report). In the back-to-back arrangement the short-pulse energy is doubled to 400 mJ.
It is worth to note, that discharge-pumped KrF amplifiers of this (20 cm^2) cross-section are not available. There are a few laboratories worldwide, where such devices are operated, however they are very complex and are only for "in-house" use; necessitating a continuous presence of the corresponding technical staff. As far as our research and development activity is concerned, our aim was to develop a short-pulse KrF amplifier, where operation – through the invention of new concept – allows a maintance-free, daily use, as a part of our high-brightness KrF laser system and to ensure the user-facility like operation of our laboratory. The photo of this amplifier is shown in Fig. 2. Further details can be found in a forthcoming publication [6], which has been sent for publication in Review of Scientific Instrument.
This amplifier is already in operation (in the process of a long-term test run); but not yet integrated into the short-pulse laser system. In this respect we are suffering some delay. Beyond the scientific "detours" of this development (UV preionized "orthogonal" approach, "internal" X-ray preionization) the main reason of this delay is connected to the large "inertia" of the necessary technical and administrative steps of the associated development activity. Beyond the development of the X-ray preionized amplifier, a similar development activity of technical feature was also necessary when integrating the novel pulse cleaning arrangement into the system, necessitating the construction of a different excimer amplifier chain (see later Fig.4, 5 in the point of "Experiments with the Nonlinear Fourier Filter").
On the other hand the main scientific goal (the realization of a gain module, offering and even surpassing the promised amplification properties) is achieved; its integration into the system – in a back-to-back form – is more technical and – based on our former experience – surely realized.

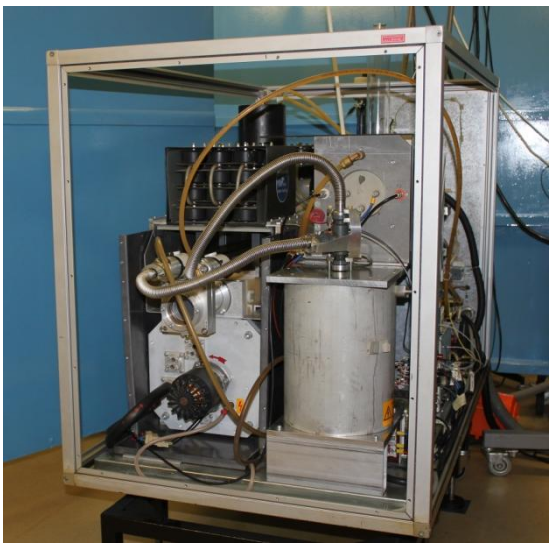

Figure 2 *Photograph of the large aperture amplifier*

Contrast issues

As the maximum intensity of laser systems is continuously increasing (recently surpassing the 10^{22} W/cm^2 level) [8, 9] an increasing interest is concentrated on the temporal and spatial quality of the pulses (beams). From the point of view of most applications the intensity level of the temporal background prior to the main pulse is of pronounced importance, since it can significantly change the nature of interaction already at a low intensity (~ 10^7 W/cm) level [10]. The necessary intensity contrast of ~ 10^{15} – deriving from these numbers – is hardly achievable by the standard laser technologies and by the available pulse cleaning techniques [11, 12].

Short-pulse KrF excimer systems have the advantage – connected to the direct amplification scheme used there – that the only source of temporal noise is the ASE [5], which shows a smooth temporal distribution however rapidly develops with increasing gain.

Experiments with the Nonlinear Fourier Filter

Recently a novel pulse cleaning method – called as Nonliner Fourier Filtering (NFF) – was introduced by us [13], whose parameters (such as maximum throughput, contrast enhancement, energy scalability) appear to be very promising.

In the frame of this project our research was concentrated on characterization and further development of the NFF. In this investigated arrangement the nonlinear component is situated in the center of a confocal telescope surrounded by a conjugated beam-block filter pair. Our research showed that the diffraction effects during the imaging process, which mostly determine and limit the achievable temporal contrast improvement to the relatively low ~ 10^3 level. [14]

We developed a computer based numerical simulation for studying the maximum achievable contrast improvement. This simulation shows that objects with sharp edges (containing high spatial frequencies) can be imaged by radiation of medium frequency only with poor contrast, which can significantly be improved by apodization (by proper control of the high spatial frequencies of the object). It was found that large variety of modulation of the spatial frequencies lead to better spatial contrasts of imaging up to 10^10. [14] Experimentally two possible realizations of such improved imaging are considered. The first is to use a specially fabricated transmission filter of the desired intensity distribution. The second is to create the desired object by an image of an optical system of low numerical aperture, completed by a second aperture blocking the low (<10^{-3}) intensity part of this picture. In Fig. 3 experimental realization of the preferred latter option is shown, which allows the use of amplifier stages as an integral part of the optical system.

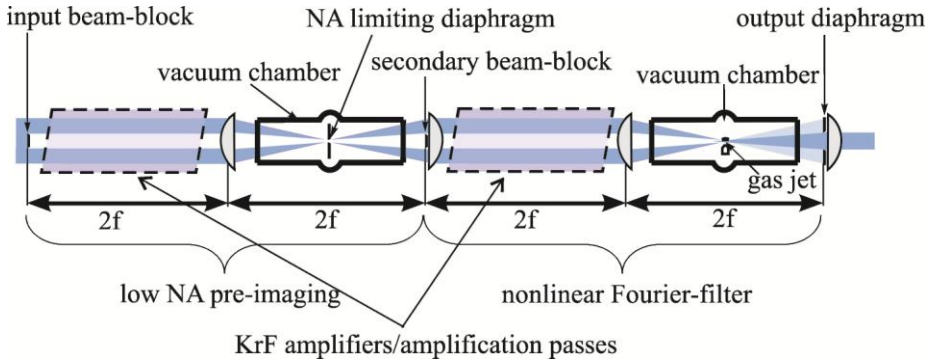

Figure 3 *Schematic of the nonlinear Fourier-filter*

This low NA pre-imaging system has threefold advantages; creates an object with reduced spatial frequency components, makes the unwanted background spatially coherent, promoting high contrast imaging and also acts as a standard spatial filter reducing ASE coupling between two amplifiers. The improved nonlinear Fourier filter was tested at the end of a KrF ultrashort pulse laser system, successfully reducing the temporal background of the output. Intensity dependent transmission measurements of the nonlinear filter showed temporal contrast improvement up to 10^5. The measurements were limited by the dynamical range of the applied photodiodes. The achievable spatial contrast of imaging using low NA pre-imaging was further studied – using a modulated diode laser and a phase-sensitive detection – in a measurement of extended dynamical range. Using this arrangement the background in the image plane was found to be still lower than the detection limit, giving an indirect proof of $>10^7$ contrast improvement [14].

The additional losses in energy of this improved setup require further amplification of the filtered beam. Therefore a KrF system of three amplifier stages has been built [15]. This required complete restructuring of the hybrid dye-excimer laser system. Previously the XeCl pump laser and the short-pulse KrF amplifier were pumped by a common pump circuit, which was then completed by an – externally synchronized – KrF final amplifier. In the new arrangement, realized during the project, a double-discharge KrF amplifier – matched to the optical and geometrical requirements of the NFF – is developed, which was externally synchronized to the XeCl pump laser and to the KrF final amplifier by an in-house designed three-stage active synchronization unit. This unit was responsible to compensate for the long-time drifts of the lasers. Fig. 4 shows the schematic of the high-contrast high-brightness KrF laser system including their synchronization and the way how the NFF is integrated into the system. In Fig. 5 the corresponding photograph of the system is shown [15].

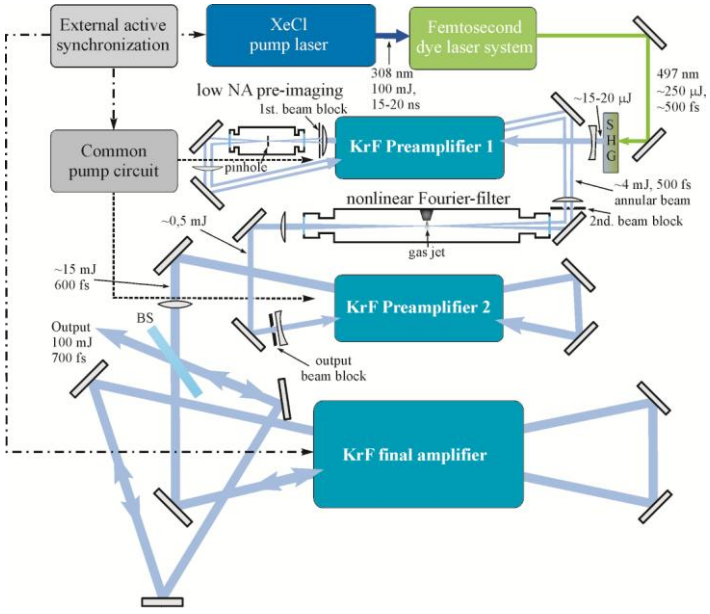

Figure 4 *Schematic of the high-contrast, high-brightness KrF laser system*

Figure 5 *Photograph of the high-contrast, high-brightness KrF laser system*

After the temporal filtering the second KrF pre-amplifier is used in a double pass arrangement to boost up the energy to the level desired by the final amplification stage. The final amplification stage having an effective cross section of ~4x4 cm^2 is used in a double pass two beam multiplexing arrangement. This setup gives access to higher portion of the energy stored in the amplifier.
With the system we produced short pulses of 100 mJ energy, ~700 fs pulse duration (positively chirped), ~2 times limited by diffraction (corresponding to 10^{20} $Wcm^{-2}sterad^{-1}$) and 10^{11} focused intensity contrast. (In case of 50 mJ output, 10^{12} intensity contrast could be obtained.) This laser system with its unique parameters gives access to laser-matter interaction experiments at 10^{19} W/cm^2 intensity level with high contrast at 248 nm. Presently it acts as a workhorse of the HILL laboratory in the frame of the access programme of the Laserlab Europe IV project [15].
It is worth to note/emphasize that the contrast improvement of NFF (>10^7) is far superior compared to the other methods. The inclusion of this pulse cleaning technique into our high-brightness system further increases the number of unique parameters of our system [13, 14, 15].
The impact of this development – strongly connected to the achievements of the present OTKA project– is already visible by receiving invitations to the participation in review articles [16] and books [17].

Limits of the temporal contrast offered by NFF

If one compares the (experimentally proven) contrast improvement of NFF (>10^5 in the UV) to the ratio of the new and the former intensity contrast of our short-pulse KrF laser system (~10^2), it is clearly seen that the latter value is significantly below the theoretically achievable one. Our investigations proved this to be connected to the contribution of the ASE generated in the amplifier chain following the NFF stage. Former times the gain in a KrF amplifying medium was known to be the same for long and short pulses – assumed to be influenced only by saturation of amplification and absorption – therefore having minor contribution to the deterioration of the contrast. Detailed study of this matter [18] pointed out, that the number of excited particles (molecules) available for pulses of different durations can be significantly different [17, 18].
The dependence of the extractable energy of excimers on the pulse duration was already recognized and studied in early publications [19, 1]. That time this dependence was attributed to the possible effects of the reabsorption of the transiently populated ground state (X) and of the relaxation of the excited state (B) [19], without defining their relative contribution. Exploration of the latter question,

however, becomes possible by comparing the saturated and unsaturated amplification properties of excimers for different pulse durations [17, 18]. With this "extended" treatment of the experimentally observed amplification properties the relative contribution of both the X and B states can be determined, leading to the characterization of material constants, like relaxation time of the B state, dissociation time of the X state, the transient absorption coefficient of the short-living ground states (σ_a) for the different excimers. Details of this study – from the practical point of view of the maximum achievable temporal contrast – can be found in [17, 18].

Plasma-mirror experiments

One of the ultimate methods of contrast improvement of ultrashort laser pulses is the plasma mirror technique [11]. Plasma mirrors have been broadly applied for infrared solid state systems. In case of short wavelength KrF lasers the larger penetration depth is expected to limit the reflectivity. This may significantly reduce the energy throughput. Our investigations showed, however, that both for 220 fs and 500 fs KrF pulses it is possible to obtain as high to 70% reflectivity with the optimized ~12°angle of incidence [20]. The results are shown in Fig. 6. It is found crucial that the incoming beam mus have good beam quality and modest prepulse level, which does not modify the target. For an efficient plasma mirror operation the intensity of ASE prepulse on the plasma mirror target must be less than 10^7 W/cm^2. When an antireflection-coated quartz plate is used as a target the reflectivity increased until 10^{15} W/cm^2 intensity and then saturated. Due to the low intensity reflection of the antireflection coating it allows two orders of magnitude contrast improvement. The detailed study of the reflected beam showed that its spatial quality is high; it can be focused to the same spotsize as the original beam. The spectrum of the reflected beam shows a Doppler shift, the spectrum, however remains within the gain curve of the KrF amplifier. Consequently the plasma mirror can be applied befor the final amplifier, when the contrast and quality of the incident beam is high enough to obtain optimum operation of the plasma mirrors and the final amplifier can compensate for the energy loss of temporal filtering. The obtained results could well be explained [21] by the classical Drude-model [22], a new arrangement for its integration to the present laser system is suggested, too.

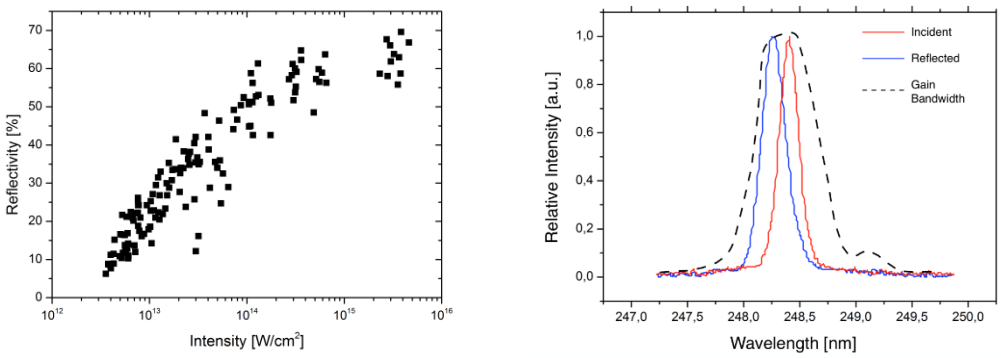

Figure 6 *The intensity dependence of the reflectivity for s-polarized beam of 500 fs duration and the measured spectral shift as compared with the gain bandwidth.*

Dependence of plasma-reflection on the contrast of the beam

As the NFF was integrated into our KrF laser system, ~12 order of magnitude temporal intensity contrast could be obtained. The new SORL focusing off-axis parabola allowed to obtain intensities up to 1.5*10^{18} W/cm^2 with a 10^6 W/cm^2 (ASE) prepulse level. Thus no preplasma, even no significant number of photoionized ions [10] were present at the arrival of the main pulse. Under these conditions we investigated the reflected radiation as well. According to the expectations the reflectivity is decreasing with increasing intensity, as shown in Fig.7a). The reflectivity is higher in the case of the low contrast beam, probably due to the Raman scattering and other nonlinear phenomena in the preplasma, whereas the high intensity radiation was absorbed in the case of an initially steep vacuum-solid surface. This behaviour was similar both for low-Z (boron) and high-Z

(Au) targets. Simultaneously with the reflectivity measurements the total x-ray emission was also studied using an Al- filtered X-ray diode. An increased X-ray conversion was found with the absorbed energy which is proportional to $I_{abs}^{1.65}$.
The spectral behaviour of the reflected radiation has an interesting feature which is shown in Fig. 7 b). In the studied intensity range a blue spectral shift is attributed to the opposite propagation to the laser beam, which increased and then saturated at the highest intensities. The highest Doppler shift can be observed at the highest intensity and contrast level of the incoming beam, in agreement with earlier observations of other groups [23]. Our intensity and contrast however was higher than therein, thus the velocity up to $5*10^7$ cm/s can be derived from the maximum Doppler shift, corresponding to an acceleration of $1.5*10^{18}$ m/s^2. As this acceleration is attributed to block acceleration [24] of macroscopic matter, it is also higher than the results in previous works. Note, that our intensity was still well below the relativistic limit, due to the short wavelength of the KrF laser. This is the reason that we could not observe red Doppler shift, which appears in the relativistic case (when the **v**x**B** force starts to dominate). For the same reasons and due to the observed saturation of the Doppler shift at the highest intensities, we can state that we observed the highest possible acceleration of plasma blocks in the direction opposite to the laser beam.
In conclusion:

- First experiments were carried out with the high contrast (10^{12}) KrF laser system.
- Record high blue shift was observed from the plasma propagating opposite to the laser beam.
- The observed 1.6 10^{18} g acceleration is the highest „block acceleration" (higher than that observed in earlier experiments due to the high contrast of the laser beam).
- The high intensity results can be explained mainly by the Brunel absorption, but detailed simulations are needed.
- In case of the Brunel absorption high harmonics are expected up to the CWE limit, higher than the formerly seen 2-4ω radiation.
- Different dependence of the reflectivity and of the Doppler shift on the intensity is observed for low-contrast and high-contrast pulses (see Fig. 7).

As the intensity and contrast parameters of our improved KrF pump laser are unique; these results are new, they are under evaluation at present. We are preparing three publications on this topics in high quality journals [25], one oral presentation is due to the end of January at the 40th PHEDM Hirschegg Workshop [26], and a poster at the Royal Society in early March.

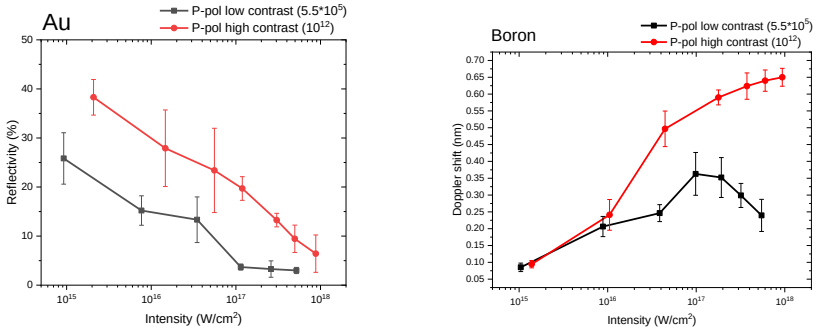

Figure 7 *Intensity dependence of reflectivity from gold target in case of low (black) and high contrast (red), pump radiation and intensity dependence of the Doppler shift from boron target.*

Study of noble gas clusters

In our future plans – aiming the use of our high-brightness KrF system for the generation of intense X-ray radiation at ~2Å wavelength [5] – noble gas clusters as the most efficient target play a central role. The efficiency of the wavelength conversion is a critical function of the characteristics of the target, like the cluster size, density etc. In this respect the study of the effect of the geometry of the valve, the backing pressure, and of the recombination process is of crucial importance. Our

corresponding investigations showed that the recombination process is dominated by atom-to-itself recollisions irrespective of cluster size and material. [27]

Pump-probe measurements

By slight modification in the KrF laser system we made it temporally tunable from 150 fs to 2 ps in 4-5 steps. This was realized by using BBO crystals of different length for frequency doubling and a diffraction grating-based pulse compressor.

It is known that different characteristic time belongs to different excitation or energy coupling processes. Since these processes are also responsible for the technologically interesting periodic surface structure formation, the study of their dynamics is of both scientific and practical importance.

As the first step we made laser matter interaction experiments using KrF laser pulses of two different (250 and 480 fs) durations on amorphous carbon, silicon and tinanium. As a result, different surface patterns were obtained where the periodicity and the complexity of the surface texture were also dependent on the pulse durations [28-30].

Laser induced periodic surface structures were created on Si (100) and Si (111) wafers by 500 fs laser pulses at 248 nm. The period of the created grooves varied between 1.1 μm and 3.3 μm. Accumulation effects were observed by investigating the dependence of the regularity of grooves on the number of irradiated pulses. The observations supported the advantage of the use of UV femtosecond pulses for this type a surface modification like for micro-machining; the short wavelength allows to create μm sized structures and strong absorption (even in materials which are transparent in the visible or near IR range) [31].

The measurement of transient optical properties allows better understanding of the nature of laser induced processes. Conventional ellipsometry is not capable of following changes in the subnanosecond timescale. Combining the pump-probe technique with a single wavelength null-ellipsometry, we could follow the optical changes of silicon with ps time resolution. Different laser intensities and delay times between the 496 nm probe and 248 nm pump pulses are used in the experiments. It is shown that besides thermal effects, the in depth free charge carrier distribution and their electron-phonon relaxation time has to be taken into account in the frame of the two-temperature model. Numerical temperature calculations indicate the decay of temperature in 10 ps time range.

The imaging nature of our pump-probe null-ellipsometer gives the possibility to study local diffusion of charge carriers in abruptly excited materials [32].

Generation of intense sub-terahertz radiaton with short-pulse KrF lasers

THz waves – whose frequency range is from 0.1 to 10 THz – can penetrate and image inside plastics, semiconductor wafers, fabrics, and most dielectric materials that may be opaque to visible light, have low photon energies that do not cause harmful photoionization in biological tissue, and exhibit strong dispersion as well as absorption for numerous molecules i.e. molecular fingerprinting. These qualities of THz radiation ensure a significant impact on 21st century science and industry. Since the need for precise control of this radiation is far too great [33, 34], parallel investigations have begun in this direction. Out of the few laser to THz energy conversion methods, the PCA (Photoconductive Antennas) [35] with its relative ease of use supply a perspective method for the generation of intense terahertz radiation.

The basis of the phenomena is that laser photons excite the carriers in to the conduction band and an external bias field accelerates the carriers. The resulting transient photocurrent is the source for the terahertz radiation. Some efforts to increase the terahertz yield are based on the increase of the antenna's aperture. Another strategy is to increase the bias voltage for which the limiting factor is the substrate material's breakdown voltage [36]. This value strongly depends on the substrate's band gap, which the laser photons excite. Historically GaAs substrates were used with a band gap of 1.44eV and with a relatively low breakdown voltage (around 10kV cm-1). The straightforward next

step in this direction is to find a material with a wider band gap that we can still excite with our short-pulse KrF laser of high photon energy (5 eV) [37, 38, 39].
During 2017 we tested many large band gap semiconductor substrates, of which silicon carbide PCAs yielded the highest THz pulse energies. Then large aperture (5 cm x 5 cm) PCAs were fabricated from 4H- and 6H-SiC and record THz pulse energies (22 μJ) were demonstrated with this technique at 30 $kVcm^{-1}$ in vacuum. Using 80 mJ energy of our short-pulse KrF laser system, strong dependence of the THz generation yield on the bias electric field – without any sign of saturation – was found. Strong correlation was observed between the THz yield and the laser energy contrast for reasons that are still under investigation (Fig. 8b).

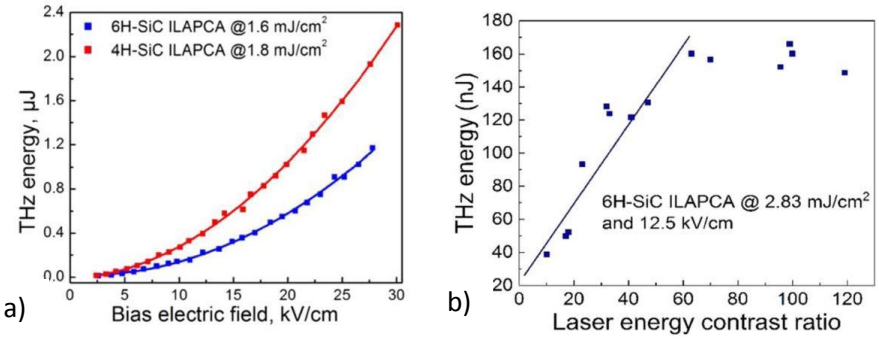

Figure 8 *Dependence of the THz energy on the bias electric field (a), and on the temporal contrast of the pump beam (b)*

In order to increase the bias electric field and avoid breakdown a high-voltage, short pulse power-supply was developed by us for dynamic bias-field generation. Since high electric fields (>30 kV/cm) were applied, which are well above the breakdown limit in air, the experiments were carried out in vacuum. Energies up to 11 μJ were obtained for the quasi-half-cycle pulses in the far-field, using a special interferometric quartz mask. A THz Michelson-interferometer was built for pulse characterization. The central frequency-component was ~0.1 THz with a pulse duration of ~5 ps and an overall narrow bandwidth. This makes this pulse ideal for excitation/acceleration purposes, and for any other application that requires a large ponderomotive potential. As an application of this source, the nonlinear THz transmission of an InGaAs sample was measured, using a Z-scan arrangement. An increase of transmission of 1.6 was observed in the focus, which corresponds to an electric field strength of ~60 kV/cm. New, larger and more durable antennas are under consideration, as well as quartz coated antennas to avoid the use of vacuum systems in the future.

<u>Accelerated photodegradation of biopolymers</u>

One of the candidates for the most widely usable biodegradable, versatile polymers of the incoming decades is PLA (Polylactic acid). A common testing procedure for degradation is based on the use of a so called weather-chamber; to substitute the impact of UV radiation, weather etc. on the samples at an order of 10-100. Some important industrial and scientific applications require the finish in a timely fashion of these tests (less than month timescale).
Our method provides an even more accelerated (~10^9) photodegradation with this material at this wavelength [40]. We compared and matched the total absorbed photon energies emitted by the xenon lamp of the weather chamber, and by our KrF (248 nm) laser pulses.
We analyzed the mass spectrometer, and thermogravimetric data regarding the average polymer chain lengths and found a close to linear dependence of degradation i.e. chain shortening for the total absorbed laser energy (Figure 9).
In these interactions, we presume only chemical degradation, as the KrF laser's photon energy is well above most of the PLA chain's chemical bond energies.
These investigations led to the ongoing experiments to understand this phenomenon with UV fluorescence spectroscopy, as well as with short-pulse (500fs) KrF lasers.

Possible industrial applications include: large scale precise control of polymer chain lengths, pharmaceutical applications (absorption of medicinal agents at different parts of the digestive system), more clear understanding of the behaviour of environmentally friendly materials at natural conditions.

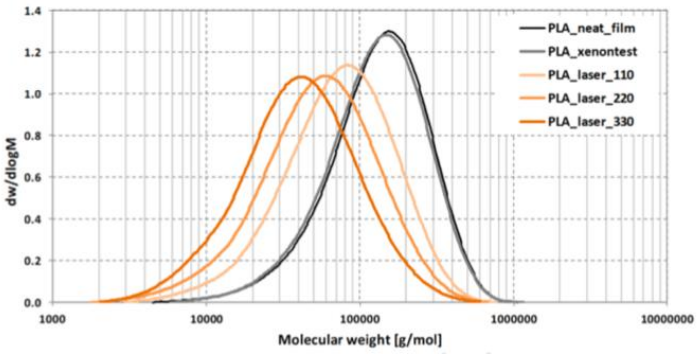

Figure 9 *Molecular weight distribution of the irradiated PLA samples*

References

(The publications which contain the results of present project are in bold type; including those ones which are before submission, submitted and published but do not contain the OTKA acknoledgement for administrative reason.)

1. S. Szatmári, G. Marowsky and P. Simon, *Femtosecond excimer lasers and their applications,* Landolt–Börnstein - Group VIII **1B1** (Eds. G. Herziger, H. Weber, R. Poprawe), 215 (2007).
2. S. Szatmári, F.P. Schäfer, E. Müller-Horsche, W. Mückenheim, *Hybrid dye-excimer laser system for the generation of 80 fs, 900 GW pulses at 248 nm,* Optics Communications **63**, 305 (1987).
3. R. Nodomi, Y. Oeda, K. Sajiki, S. Nakajima, M. Watanabe, S. Watanabe, *High repetation rate, wide-aperture KrF lasers for subpicosecond amplification,* IEEE Journal of Quantum Electronics **27**, 441 (1991).
4. S. Szatmári, G. Almási, P. Simon, *Off-axis amplification scheme for short-pulse amplifiers,* Applied Physics B **53**, 82 (1991).
5. A. B. Borisov,C. J. McCorkindale, S. Poopalasingam, J. W. Longworth, P. Simon, S. Szatmári and C. K. Rhodes, *Rewriting the Rules Governing High Intensity Interactions of Light with Matter,* Reports on Progress in Physics 79, 046401 (2016).
6. **S. Szatmári, *Short-pulse KrF amplifier using spatially-tunable X-ray preionization*, Review of Scientific Instruments (submitted in 2019 december)**
7. H. Shields, *X-ray preionization technology for high pressure gas discharge lasers,* SPIE Proceedings **1046**, 15 (1989).
8. Tae Moon Jeong and Jongmin Lee, Femtosecond petawatt laser, Annalen der Physics **526**, 157 (2014)
9. Y. Chu, X. Liang, L. Yu, Y. Xu, L. Xu, L. Ma, X. Lu, Y. Liu, Y. Leng, R. Li, and Z. Xu, *High-contrast 2.0 Petawatt Ti:sapphire laser system,* Optics Express **21**, 29231 (2013).
10. Földes, I. B., Bakos, J. S., Gál, K., Juhász, Z., Kedves, M. A., Kocsis, G., Szatmári, S. and Veres, G. *Properties of high harmonics generated by ultrashort UV laser pulses on solid surfaces*, Laser Physics **10** (1), 264 (2000)
11. H. C. Kapteyn, M. M. Murnane, A. Szoke, and R. W. Falcone, Prepulse energy suppression for high-energy ultrashort pulses using self-induced plasma shuttering, Optics Letters **16** (7), 490–492 (1991)

12. Y. Xu, Y. Leng, X. Guo, X. Zou, Y. Li, X. Lu, C. Wang, Y. Liu, X. Liang, R. Li, and Z. Xu, Pulse temporal quality improvement in a petawatt Ti:Sapphire laser based on cross-polarized wave generation, Optics Communications **313**, 175–179 (2014)

13. **S. Szatmári, R. Dajka, A. Barna, B. Gilicze, and I. B. Földes, *Improvement of the temporal and spatial contrast for high-brightness laser beams,* Laser Physics Letters 13(7), 075301 (2016)**

14. **B. Gilicze, R. Dajka, I. B. Földes, and S. Szatmári, *Improvement of the temporal and spatial contrast of the nonlinear Fourier-filter,* Optics Express 25 (17), 20791–20797 (2017)**

15. **Gilicze, B., Homik, Zs., Szatmári, S. *High-contrast, high-brightness ultraviolet laser system* Optics Express 12: 17377-17386 (2019)**

16. **Colin N. Danson, Constantin Haefner, Jake Bromage, Thomas Butcher, Jean-Christophe F. Chanteloup, Enam A. Chowdhury, Almantas Galvanauskas, Leonida A. Gizzi, Joachim Hein, David I. Hillier, Nicholas W. Hopps, Yoshiaki Kato, Efim A. Khazanov, Ryosuke Kodama, Georg Korn, Ruxin Li, Yutong Li, Jens Limpert, Jingui Ma, Chang Hee Nam, David Neely, Dimitrios Papadopoulos, Rory R. Penman, Liejia Qian, Jorge J. Rocca, Andrey A. Shaykin, Craig W. Siders, Christopher Spindloe, Sándor Szatmári, Raoul M. G. M. Trines, Jianqiang Zhu, Ping Zhu, and Jonathan D. Zuegel, *Petawatt and exawatt class lasers worldwide, High Power Laser Science and Engineering,* Vol. 7, e54 (2019)**

17. **S. Szatmári, *High-brightness excimer lasers and extreme condition they produce,* Handbook of Laser Technology&Application 2nd. Edition (invited contribution, in press)**

18. **S. Szatmári, R. Dajka, B. Gilicze , Zs. Kovács and I. B. Földes, *Generation of intense and temporally clean pulses; Contrast issues of excimer and CPA systems,* (manuscript planned to be published in Laser Physics)**

19. S. Szatmári, F.P. Schäfer, *Comparative study of the gain dynamics of XeCl and KrF with subpicosecond resolution*, J. Opt. Soc. Am. B 4, 1943-1948 (1987)

20. **B. Gilicze, A. Barna, Z. Kovács, S. Szatmári, and I. B. Földes, *Plasma mirrors for short pulse KrF lasers,* Rev.Sci. Instrum. 87(8), 083101 (2016)**

21. **István B Földes, Barnabás Gilicze, Zsolt Kovács and Sándor Szatmári, *Plasma Mirrors for Cleaning Laser Pulses from the Infrared to the Ultraviolet,* EPJ Web of Conferences 167, 04001 (2018)**

22. R. Fedosejevs, R. Ottmann, R. Sigel, G. Kühnle, S. Szatmári, F.P. Schäfer, *Absorption of subpicosecond ultraviolet laser pulses in high-density plasma*, Appl. Phys. B 50, 79 (1990)

23. R. Sauerbrey, *Acceleration in femtosecond laser-produced plasmas*, Physics of Plasmas 3, 4712 (1996)

24. H. Hora et al., *Pressure of picosecond CPA laser pulses substitute ultrahigh thermal pressures to ignite fusion*, High Energy Density Physics **35**, 100739 (2020)

25. **Zs. Kovács, B. Gilicze, K. Bali1, S. Szatmári, I. B. Földes, *Large spectral shift of reflected radiation from laser plasmas generated by high contrast KrF laser pulses*, Frontiers in Physics – Interdisciplinary Physics (accepted for publication upon the abstract)**

26. **Zs. Kovács, B. Gilicze, K. Bali, S. Szatmári and I.B. Földes, *Reflectivity and spectral shift from plasma mirrors generated by KrF laser,* 40th Hirschegg Workshop, 2020. January, (oral presentation)**

27. **B. Bódi, M. Aladi, P. Rácz, I.B. Földes and P. Dombi, *High Harmonic generation on noble gas clusters*, Optics Express 27 26721 (2019)**

28. **J. Csontos, Z. Toth, Z. Pápa, J. Budai, B. Kiss, A. Börzsönyi, M. Füle, *Periodic structure formation and surface morphology evolution of glassy carbon surfaces applying 35-fs–200-ps laser pulse,s* Applied Physics A, Volume 122, Issue 6, 593 (2016)**

29. **A. Gárdián, R. Masa, J. Csontos, J. Budai, M. Füle, Á. Börzsönyi, B. Kiss, K. Turzó, Zs. Tóth, *The influence of pulse duration, wavelength and fluence on laser induced structure formation from the viewpoint of dental applications,* The 13th Conference on Laser Ablation (COLA-2015) Cairns, Australia, 31 August – 4 September 2015 (poszter), 2015**

30. **J. Csontos, Z. Toth, Z. Pápa, J. Budai, B. Kiss, A. Börzsönyi, M. Füle, *Structure and surface morphology evolution of amorphous carbon surfaces during transformation by 0.2-20 ps laser pulses*,The 13th Conference on Laser Ablation (COLA-2015) Cairns, Australia, 31 August – 4 September 2015 (poszter), 2015**

31. **B. Gilicze, M. Moczok, D. Madarász, N. Juhász, B. Racskó, and L. Nánai,*Periodic surface structure creation by UV femtosecond pulses on silicon,* AIP Conf. Proc. 1796, 030001-1-030001-5, 2017**

32. **B. Gilicze, P.I. Szabó, Zs. Homik, M. Moczok, Zs. Kovács, Z. Tóth, L. Nánai, *Regular patterns created by femtosecond laser pulses,*TIM17 Physics Conference, 25-27 May, 2017, Timisoara, Romania (előadás), 2017**

33. Fülöp J A, Pálfalvi L, Klingebiel S, Almási G, Krausz F, Karsch S and Hebling J, *Generation of sub-mJ terahertz pulses by optical rectification*, Optics Letters 37 557 (2012)

34. Hirori H, Doi A, Blanchard F and Tanaka K, *Single-cycle terahertz pulses with amplitudes exceeding 1 MV/cm generated by optical rectification in $LiNbO_3$*, Applied Physics Letters 98 (9) 10.1063 (2011)

35. You D, Jones R, Bucksbaum P H, Dykaar D R, *Generation of high-power sub-single-cycle 500-fs electromagnetic pulses*, Optics Letters 18 (4) 290 (1993)

36. Stone M R, Naftaly M, Miles R E, Fletcher J R and Steenson D P, *Electrical and radiation characteristics of semilarge photoconductive terahertz emitters*, IEEE Trans. Microw. Theory Tech. 52 (10) 2420 (2004)

37. **X. Ropagnol, Z. Kovacs, B. Gilicze, M. Zhuldybina, F. Blanchard, S. Szatmari, I.B. Foldes, et T. Ozaki,. 2019. *Intense sub-THz radiation from wide bandgap photoconductive antenna excited by UV laser beam*, Affiche présentée lors de la conférence : Optical Terahertz Science and Technology (Santa Fe, NM, USA, March 10-15, 2019). poster**

38. **X. Ropagnol, Zs. Kovács, B. Gilicze, I. Földes, S. Szatmári, T. Ozaki, *Generation of Terahertz radiation Using Large Aperture Photoconductive Antennas and Subps KrF Lasers,* Atto 2019, Szeged, poster, No. 267**

39. **X Ropagnol, Zs Kovács, B Gilicze, MZhuldybina, F Blanchard, CMGarcia-Rosas, S Szatmári, I B Földes and T Ozaki, *Intense sub-terahertz radiation from wide-bandgap semiconductor based large-aperture photoconductive antennas pumped by UV lasers*, New J. Phys. 21 113042 (2019)**

40. **K. Litauszki, Zs. Kovács, L. Mészáros, Á. Kmetty, *Accelerated photodegradation of poly(lactic acid) with weathering test chamber and laser exposure – A comparative study,* Polimer Testing 76, 411-419 (2019)**